

Bistable tuned mass damper for suppressing the vortex induced vibrations in suspension bridges

Saman Farhangdoust^{*1}, Pejman Eghbali² and Davood Younesian²

¹Department of Civil and Environmental Engineering, Florida International University, Miami, FL 33174, USA

²School of Railway Engineering, Iran University of Science and Technology, Tehran 16846-13114, Iran

(Received April 24, 2019, Revised January 22, 2020, Accepted February 4, 2020)

Abstract. The usage of conventional tuned mass damper (TMD) was proved as an effective method for passive mitigating vortex-induced vibration (VIV) of a bridge deck. Although a variety of linear TMD systems have been so far utilized for vibration control of suspension bridges, a sensitive TMD mechanism to wind spectrum frequency is lacking. Here, we introduce a bistable tuned mass damper (BTMD) mechanism which has an exceptional sensitivity to a broadband input of vortex shedding velocity for suppressing VIV in suspension bridge deck. By use of the Monte Carlo simulation, performance of the nonlinear BTMD is shown to be more efficient than the conventional linear TMD under two different wind load excitations of harmonic (sinusoidal) and broadband input of vortex shedding. Consequently, an appropriate algorithm is proposed to optimize the design parameters of the nonlinear BTMD for Kap Shui Mun Bridge, and then the BTMD system is localized for the interior deck of the suspension bridge.

Keywords: bistable tuned mass damper (BTMD); nonlinear vibration control; wind vortex shedding; suspension bridges

1. Introduction

Wind forces cause aerodynamic instability of suspension bridge structures resulting in failures that need to be considered for bridge design and assessment (Andersen and Brandt 2018). Tacoma Narrows in 1940 in Washington, Brighton Chain Pier in 1836 in England, and Wheeling in 1854 in West Virginia are some examples of suspension bridges being destroyed because of the aerodynamic instabilities and uncontrolled oscillations (Arioli *et al.* 2015, Steinman 2017). Hence, monitoring and controlling of the wind-induced structural motions receive very much attention nowadays because of periodic hurricanes occur in many parts of the world. A wide variety of numerical and mathematical approaches have been used for structural health monitoring (SHM) of bridge structures (Farhangdoust and Mehrabi 2019, Zhou *et al.* 2018, Soman *et al.* 2018, Xu 2018, Feng *et al.* 2018, Saha *et al.* 2018). In the literature, vortex shedding, flutter, buffeting, and galloping can induce aerodynamic instabilities leading to suspension bridge collapses as a consequence of wind-bridge interaction (Larsen and Larose 2015, Guo *et al.* 2019, Vaz *et al.* 2018, Azzi *et al.* 2018). The dynamic response of Kap Shui Mun Bridge in Hong Kong has been modeled by Zhang *et al.* (2012) in which vortex shedding, flutter, and buffeting have been addressed as the load excitations. Vortex shedding is recognized as an undesirable aeroelastic phenomenon of the wind-bridge interaction which potentially causes large dynamic oscillations in the

suspension bridges (Gazzola 2015, Simiu 2011, Larsen *et al.* 2000). Vortex shedding results from rolling-up of the separating shear layers of a bluff body alternately on each side of structure gives rise to fluctuating lift forces. A large number of articles have been published on the vortex-induced oscillation of engineering structures (Wang *et al.* 2018, Munir *et al.* 2018). The structure will resonate and its oscillations will become self-sustaining if the frequency of vortex shedding matches structure's fundamental frequency (Li *et al.* 2011, Fujino and Yoshida 2002). Vibration analysis of suspension bridge deck subjected to the vortex shedding instability has been a concern to engineers because of the associated bridge failure experienced (Laima *et al.* 2014, Wang *et al.* 2018). In order to tackle the aerodynamic instability of suspension bridge structures, various teams and researchers have put their concentrations on figuring vortex-induced vibrations out (Zhang *et al.* 2008). A single-side pounding tuned mass damper was implemented by Wang *et al.* (2018) to mitigate vortex-induced vibrations of a bridge deck. They experimentally investigated the proposed TMD performance and concluded that the maximum response of their model was reduced by 94% using the TMD with mass ratio of 2%. Due to different given Reynolds numbers, VIV performance has been studied for twin-box bridge sections of Great Belt East Bridge and the Stonecutters Bridge by Zhang *et al.* (2008). Smith (2008) studied dynamic response of Wye Bridge which is a cable stayed box girder bridge with length span of 235 m. They measured the dominant frequencies of wind-induced vibration and studied the effect of vortex shedding excitation on fatigue life of the bridge structure. Field measurements of a twin steel box girder suspension bridge with a center span of 1650 m have been implemented

*Corresponding author, Ph.D Candidate
E-mail: sfarh006@fiu.edu

by Li *et al.* (2011) using the pressure sensors. The vertical vortex-induced resonance of the bridge deck has been assumed to be perpendicular to the longitudinal bridge axis. Based on the experimental data, Wu *et al.* (2013), developed two advanced nonlinear aero-elastic analysis frameworks for cable-stayed bridges using the artificial neural network and Volterra series-based models. Torsional divergence and flutter in two different suspension bridges under aeroelastic forces were modeled and analyzed by Arena and Lacarbonara (2012) using a fully nonlinear model. More recently, Zhou *et al.* (2018) presented a fully integrated finite element (FE) model in time domain, for vortex induced vibration analysis of long-span twin-box girder bridges with various geometries and wind fairing shapes. Because of the low cost, versatility, and simple required instrumentation, different researches have been carried out within the conventional tuned mass dampers (TMDs) for vibration control of long-span suspension bridge decks (Zhang *et al.* 2012, Han *et al.* 2019). The feasibility of applying passive control devices to attenuate the vortex-induced oscillations along the spans of the steel twin-box-girder Rio Niterói Bridge has been numerically and experimentally investigated by Battista and Pfeil (2000). Rohman and John (2006) investigated the responses of cables and deck for a flexible long-span suspension bridge in both directions of along-wind and across-wind using a single passive and semi-TMD. A modified single-side pounding TMD has been proposed by Wang *et al.* (2018) to investigate the vibration control of VIV of a bridge deck under action of a nonlinear force. They employed a numerical optimization based on the verified impact force model to obtain simplified design formulas for the TMD systems. Some other researchers have also utilized various optimization algorithms like algorithm genetics to enhance the system's performance (Hussain *et al.* 2015, Ranjbar *et al.* 2016). Conventional TMDs have been tuned so far only for natural frequency of the suspension bridge deck, however, to get a more sensitive and better performance, there is a basic question that needs to be answered: Which mechanism of TMDs can be tuned in a broadband frequency of inputs? Using bistable mechanisms can give TMDs the ability of taking the advantages of an exceptional sensitivity to broadband inputs. Bistable systems have been used to improve power generation capability in energy harvesting devices which are for effective conversion of a wide variety of vibration excitation environments into usable electrical power (Pellegrini *et al.* 2013, Harne and Wang 2013, Leadenham and Erturk 2014, Tang and Yang 2012, Nguyen *et al.* 2013). Specifically, bistable energy harvesting applications have been utilized in many instruments for harnessing energy from vibrations of infrastructures (Farhangdoust *et al.* 2019), environment (Wang *et al.* 2018, Vocca *et al.* 2012), sound waves (Zhou *et al.* 2017) and ocean waves (Younesian and Alam 2017). This paper aims at developing a bistable tuned mass damper (BTMD) model vibration control of VIV in a suspension bridge deck. The BTMD has one unstable and two stable states in which switching between two stable states leads to more pronounced and high performance of the bridge vibration control system.

Therefore, employing the BTMD for bridge structures can be addressed as one of the most effective and practical applications among scholars in the area of vibration control applications. Two types of single and broadband frequency of vortex shedding load are applied to the bridge structure. Accordingly, a performance comparison between the nonlinear BTMD and conventional linear TMD is carried out. Consequently, an iterative algorithm is employed to optimize the design parameters of the nonlinear BTMD for Kap Shui Mun Bridge in Hong Kong which is one of the longest a cable-stayed bridge in the world.

2. Vibration theory for vortex shedding modeling

Vortex shedding is an aero-elastic phenomenon in the wind-bridge interaction which potentially causes large dynamic oscillations of suspension bridges [14-15]. The shedding of vortices on the bridge deck gives rise to fluctuating lift forces. The bridge structure will resonate if the frequency of vortex shedding (f_v) and hence the frequency of the associated lift force, matches structure's frequency (f_n). This is the case at the wind speed of U_{crit} Eq. (1), vortex shedding frequency aligns itself to the structure's frequency f_n [13]

$$U_{crit} = \frac{1}{St} f_n \quad (1)$$

In which, St is the Strouhal number which is depends on the cross section dimension D and the Reynolds number. Vortex shedding load per unit length can be then obtained by (Simiu and Yeo 2019)

$$F_v(x, t) = q(z) d(z) \tilde{C}_L \sin[2\pi f_v(z)t] \quad (2)$$

$$q(z) = \frac{1}{2} \rho U(z)^2 \quad (3)$$

where $q(z)$ denotes the velocity pressure, $U(z)$ is the mean wind velocity at height z , $d(z)$ represents the structural width, and \tilde{C}_L is the root mean square (RMS) lift force coefficient for cross sectional geometry. Wind is a turbulent flow for which the wind velocity dependence on height above the surface. According to this feature of atmospheric boundary layer (ABL), the vortex shedding load per unit length is calculated by (Simiu and Yeo 2019)

$$F_v(x, t) = q(z) d(z) C_L(z, t) \quad (4)$$

Where $C_L(z, t)$ is the nondimensional normalized lift force. Experimental tests prove that the resonant amplification will be occurred not only at the wind speed U_{crit} Eq. (1), but also at any speed within an interval [13].

$$\frac{1}{St} f_n D - \Delta U < U_{crit} < \frac{1}{St} f_n D + \Delta U \quad (5)$$

In which, $\Delta U/U_{crit}$ is of the order of a few percent and depends on cross section dimension D and the mechanical damping. U_T as the part of turbulence with periods much longer than natural vibration period of the structure has an

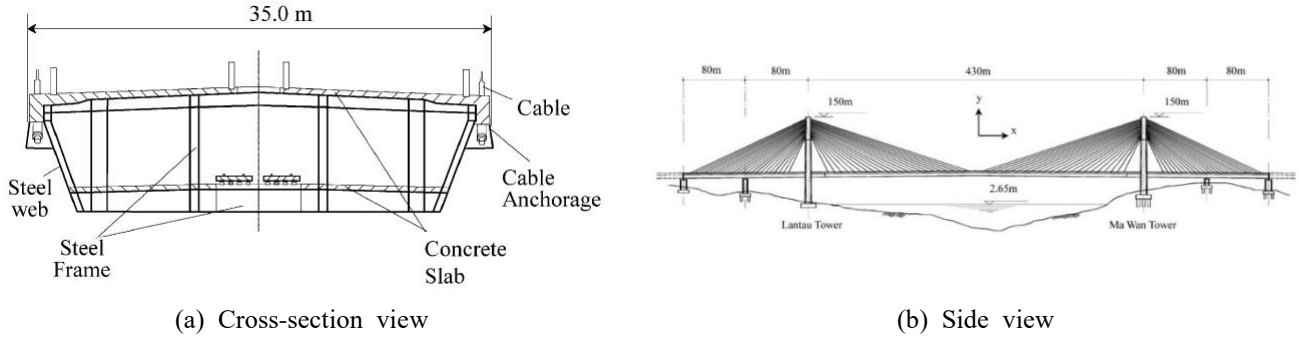
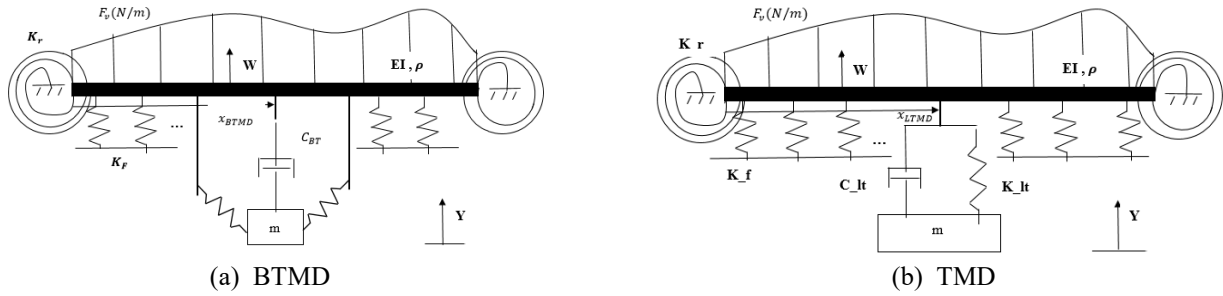

 Fig. 1 Two different views of the Kap Shui Mun Bridge (Ko *et al.* 2002), Copyright 2020, Elsevier


Fig. 2 Two schematic configuration of bridge with BTMD and TMD

essential role on shaping the broadband frequency of vortex shedding. Hence, the maximum turbulent wind speed variation from the mean speed U_T needs to be added to the mean velocity U_{crit} as a contribution to a moderately varying mean velocity of vortex shedding (Simiu and Yeo 2019). Therefore, the wind velocity of vortex shedding yield

$$f_v + f_v' = St \frac{U_{crit} + U_T}{d} \quad (6)$$

According to the ABL, to assume turbulence U_T has normal distribution is a proper approximation. The autospectrum $S_{C_L(z,t)}$ of the normalized lift force is given by (Simiu and Yeo 2019)

$$\frac{f S_{C_L(z,t)}}{\tilde{C}_L^2(z)} = \frac{f}{\sqrt{\pi} B(z) f_v(z)} \exp \left[- \left[\frac{1 - f/f_v(z)}{B(z)} \right]^2 \right] \quad (7)$$

Where $\tilde{C}_L^2(z)$ denotes the standard deviation of the C_L and $B(z)$ is spectral bandwidth which is the broadband frequency of vortex shedding. The lower and upper band of the effective frequency are respectively defined by

$$f_j^L = f_j - f_j^T = \frac{St U}{d} - \frac{St U_T}{d} = f_j \left[1 - \frac{U_T}{U} \right] \quad (8)$$

$$f_j^U = f_j + f_j^T = \frac{St U}{d} + \frac{St U_T}{d} = f_j \left[1 + \frac{U_T}{U} \right] \quad (9)$$

If the structure's natural frequency for j th mode of vibration lies on a broadband frequency between f_j^L and f_j^U , mode of vibration j will be excited by the vortex shedding. According to the friction velocity and the standard deviation for the turbulent horizontal wind

component, the maximum value of turbulent wind velocity variation is given by

$$\delta(U_T) = \frac{A U_z K}{\ln(z/z_0)} \quad (10)$$

Where z_0 is the surface roughness length which depends on terrain exposure, A is an empirical constant for the surface roughness length, K is von Karman constant, and z is the height of bridge deck above the ground. Consequently, substituting Eq. (10) into Eqs. (8) and (9), the effective frequency band of the vortex shedding can be calculated as

$$f_v^L = f_v \left[1 - \frac{\delta(U_T)}{U} \right] < f_{vortex-shedding} < f_v^U = f_v \left[1 + \frac{\delta(U_T)}{U} \right] \quad (11)$$

3. Mathematical modelling

The Kap Shui Mun Bridge is selected as the case suspension bridge for numerical simulations and mathematical modelling of BTMD. This bridge is located in Hong Kong and is known as one of the longest cable-stayed bridges in the world (Fig. 1). Interior span of the bridge with length of 430 (m) is taken as a framework along with other geometric parameters of the bridge from the records (Zhang *et al.* 2001). As it is shown in Fig. 2, the bridge is modeled by a free-free constrained Euler-Bernoulli beam with two types of BTMD and TMD.

The governing equation of motion for the bridge having a linear conventional TMD can be presented as follows

$$EI \frac{\partial^4 w}{\partial x^4} + \rho A_c \frac{\partial^2 w}{\partial t^2} + K_F * w = -Q_1(x, t) \quad (12)$$

$$Q_1(x, t) = [F_v(x, t) + C * \dot{w} + 2 * K_r * \frac{\partial w}{\partial x} + C_{LT} * (\dot{w} - \dot{Y}) + K_{LT} * (w - Y)] \quad (13)$$

$$m\ddot{Y} + C_{LT} * (\dot{Y} - \dot{w}) + k_{LT} * (Y - w) = 0 \quad (14)$$

In which, $F_v(x, t)$ is the wind force, C_{LT} and K_{LT} denote damping coefficient and stiffness of the TMD, respectively. m and C are the mass of TMD and the damping coefficient of the bridge. Parameters K_F and K_r represent respectively cables and rotational stiffness (Due to the adjacent spans). Using eigenfunction expansion (Galerkin method), one can assume

$$w(x, t) = \sum_n q_n(t) X_n(x) \quad n = 1, 2, \dots \quad (15)$$

Substituting Eq. (15) into Eqs. (14) and (16) and then implementing the orthogonality condition of the mode shapes would give

$$\ddot{q}_n(t) + 2\xi\omega_n\dot{q}_n(t) + \omega_n^2q_n(t) = -\frac{1}{M_n} \int_0^L Q_1(x, t) X_n(x) dx \quad (16)$$

$n = 1, 2, \dots$

$$\begin{aligned} \ddot{Y} + 2\xi_{LTMD}\omega_{LTMD} \left(\dot{Y} - \sum_j \dot{q}_j(t) X_j(x_{LTMD}) \right) \\ + \omega_{LTMD}^2 \left(Y - \sum_j q_j(t) X_j(x_{LTMD}) \right) = 0 \quad (17) \end{aligned}$$

$j = 1, 2, \dots$

In a same derivation procedure, the following set of nonlinear differential equations are derived in general form for the bridge deck with a BTMD system. Partial differential equations of the bridge can be obtained as follows

$$EI \frac{\partial^4 w}{\partial x^4} + \rho A_c \frac{\partial^2 w}{\partial t^2} + K_F * w = -Q_b(x, t) \quad (18)$$

$$Q_b(x, t) = [F_v(x, t) + C * \dot{w} + 2 * K_r * w' - K_{LBT} * (w - y) + C_{BT} * (\dot{w} - \dot{Y}) + K_{NBT} * (w - Y)^3] \quad (19)$$

$$m\ddot{Y} - K_{LBT} * (Y - w) + C_{BT} * (\dot{Y} - \dot{w}) + K_{NBT} * (Y - w)^3 = 0 \quad (20)$$

In which, $F_v(x, t)$ is the vortex shedding force, K_{NBT} and K_{LBT} are respectively nonlinear and linear BTMD stiffness, C_{BT} is damping coefficient of the BTMD. Accordingly, substituting Eq. (15) into Eqs. (18) and (19) and then implementing the orthogonality condition of the mode shapes would provide

$$\ddot{q}_n(t) + 2\xi\omega_n\dot{q}_n(t) + \omega_n^2q_n(t) = -\frac{1}{M_n} \int_0^L Q_b(x, t) X_n(x) dx \quad (21)$$

$n = 1, 2, \dots$

$$\begin{aligned} \ddot{Y} + 2\xi_{BTMD}\omega_{BTMD} \left(\dot{Y} - \sum_j \dot{q}_j(t) X_j(x_{BTMD}) \right) \\ - \omega_{BTMD}^2 \left(Y - \sum_j q_j(t) X_j(x_{BTMD}) \right) \\ + \frac{K_{NBT}}{m} \left(Y - \sum_j q_j(t) X_j(x_{BTMD}) \right)^3 = 0 \quad (22) \end{aligned}$$

$j = 1, 2, \dots$

Consequently, implementing the boundary conditions of free-free for the beam, one can find the mode shapes solution

$$X_n(x) = \sin\beta_n x + \sinh\beta_n x + \left[\frac{\cos\beta_n L - \cosh\beta_n L}{\sin\beta_n L + \sinh\beta_n L} \right] (\cos\beta_n x + \cosh\beta_n x) \quad (23)$$

$$\beta_n^4 = \frac{\rho A \omega_n^2 - K_F}{EI} \quad (24)$$

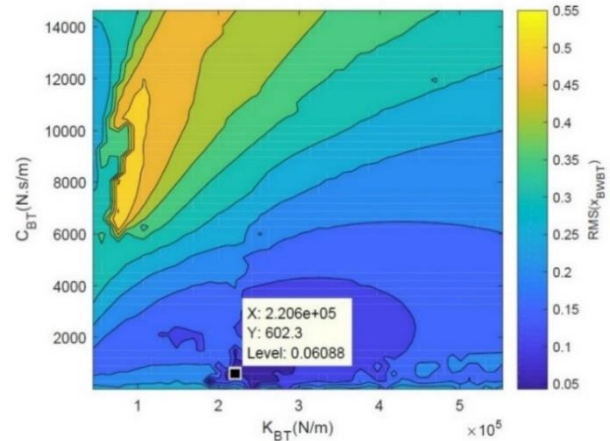


Fig. 3 Optimization map for the BTMD

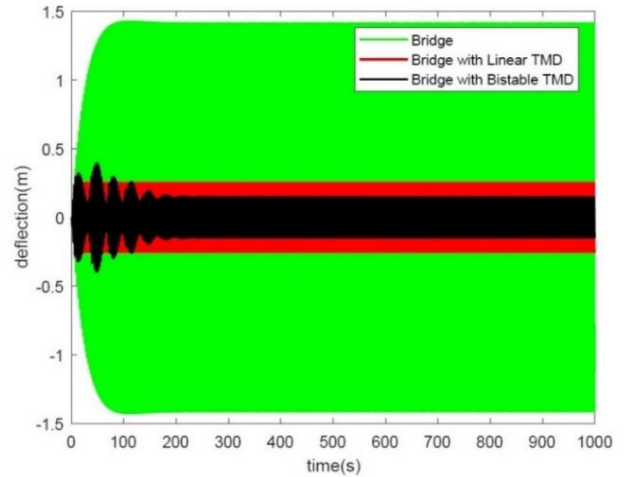


Fig. 4 Bridge deflection without TMD, with the BTMD, and with conventional linear TMD

4. Numerical results and discussion

In order to verify the proposed BTMD design, a numerical study is carried out in this section. Two scenarios are developed to evaluate the performance of TMD and BTMD systems and to examine the influence of the wind force on the vibration performance of the suspension bridge systems modeled by Fig. 2.

In the first case study, the applied force is assumed to be harmonic (sinusoidal) using Eq. (2). The mass ratio of BTMD to the bridge is taken to be 0.05. Two parameters of stiffness and damping coefficient are the design parameters that need to be optimized for getting the best performance for passive vibration controls. As it is depicted in Fig. 3, K_{NMT} and C_{MT} as the design parameters of BTMD are optimized.

The optimization map is designed in order to enhancing the BTMD performance by minimizing the VIV of the suspension bridge. Apart from that, For the conventional linear TMD, the parameters of K_{LT} and C_{LT} are also optimized and used here for making a comparison performance between the TMD and the proposed BTMD. Deflection of the different configurations of the bridge system is evaluated by Fig. 4. As a result, one can find that the deflection for the bridge system used BTMD has decreased 37% more than the system used the conventional linear TMD.

For the first scenario, the displacement of the BTMD and conventional linear TMD are also investigated in Fig. 5. The performance comparison between their displacements proves that the BMTD has a better efficiency as a passive vibration control for suppressing the VIV of suspension bridge structures.

The phase-plane diagrams are obtained for the BTMD and conventional linear TMD systems in Fig. 6. For the phase-plane of TMD, we have a trajectory in the phase-plane around the stable point which is zero (Fig. 6(a)).

For the BTMD system, we see a chaotic-like behavior for the phase-plane diagram in which the trajectory surrounds the two stable equilibrium points and results an improved performance in suppressing the VIV of suspension bridges compared with the conventional linear TMD (Fig. 6(b)).

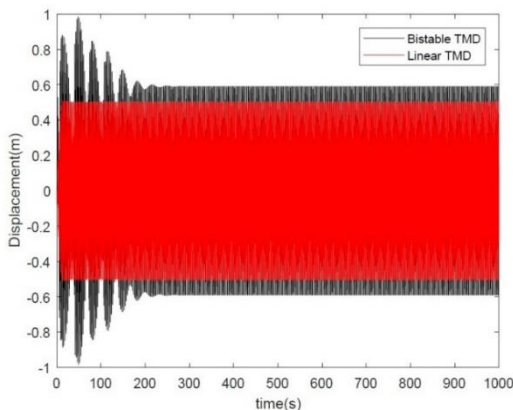


Fig. 5 Displacements of the BTMD and linear TMD

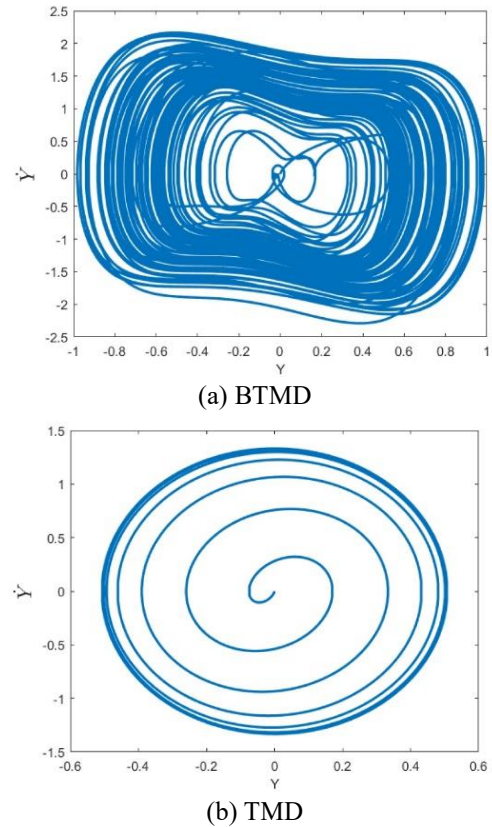


Fig. 6 Phase-plane trajectories for the conventional linear TMD and BTMD

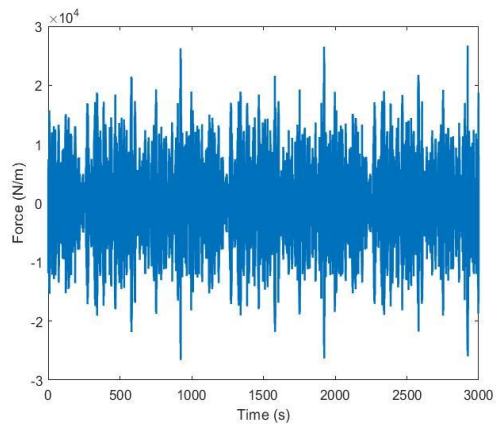


Fig. 7 Random loading generated by the Monte Carlo simulation

For the second case study, a broadband input is considered using Eq. (4) for the applied force. Toward this goal, by use of the spectral density of the wind force and Monte Carlo simulation, a typical load pattern has been generated over the bridge deck. Time history of the wind leading is presented in Fig. 7. Similar to the first case study, an optimization map is developed for designing K_{NMT} and C_{MT} as the design parameters of the BTMD (Fig. 8).

The numerical results in Fig. 9 show that the conventional linear TMD has a better performance in suppressing the VIV of the suspension bridge in comparison with the BTMD if and only if a narrow band of wind speed

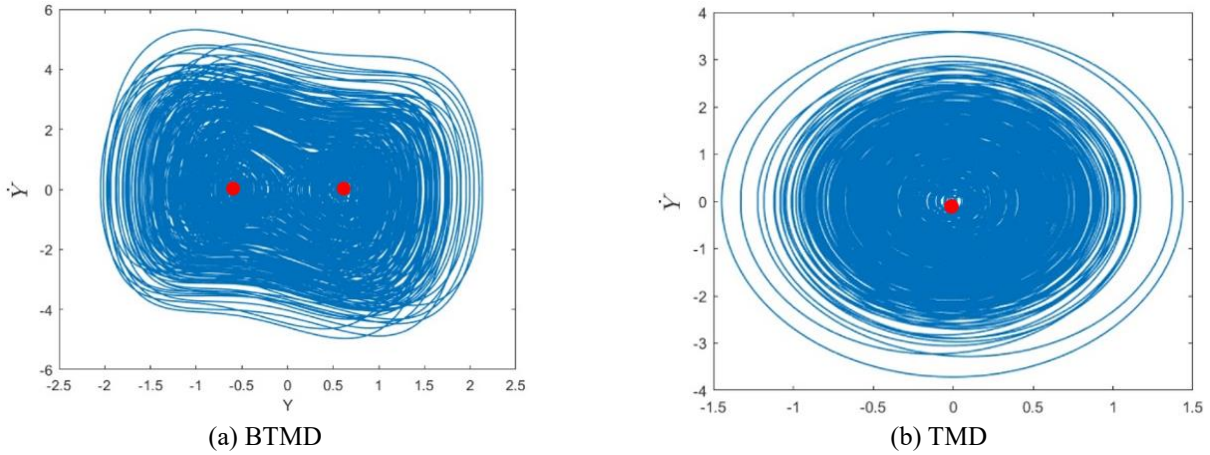


Fig. 8 Phase-plane trajectories for the conventional linear TMD and BTMD

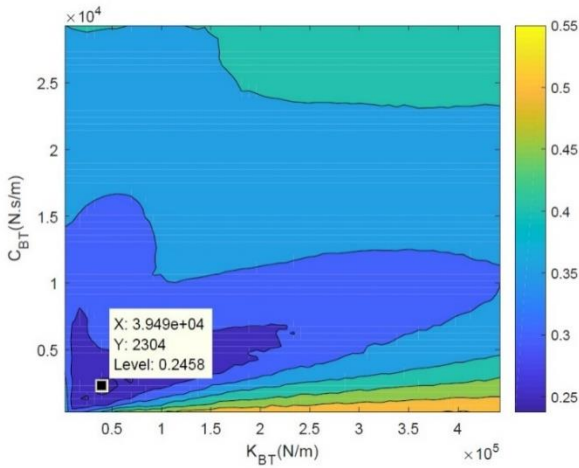


Fig. 9 Optimization map for the BTMD

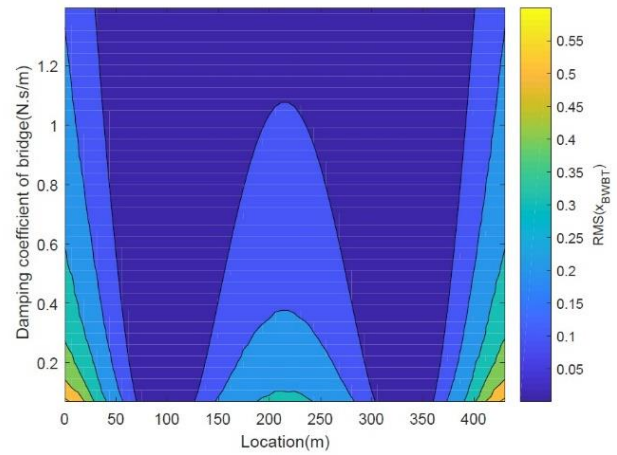


Fig. 11 The performance map of using BTMD for the interior bridge deck

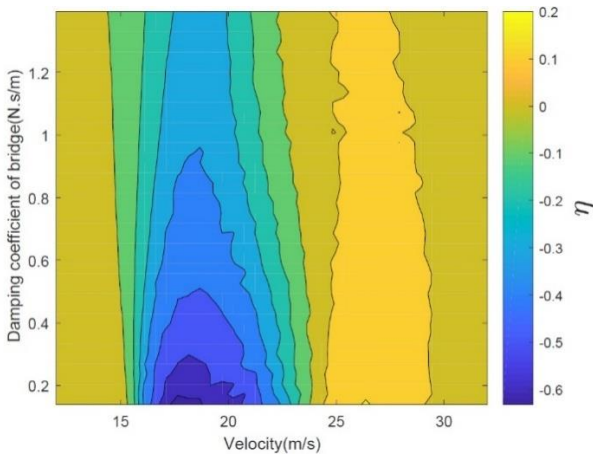


Fig. 10 Comparison performance between BTMD and TMD in different bands of input

(16 to 23 m/s) is considered for the vortex shedding velocity U_{crit} Eq. (1). However, as experimental tests demonstrate the resonant amplification is occurred at any speed within a broadband input of vortex shedding velocity (Eq. (5)) [13], the numerical results for this condition illustrate the BTMD system has the most optimal performance compared with the conventional linear TMD.

η defined as an improvement indicator for the bridge vibration control system by:

$$\eta = \frac{RMS(x_{BWBT}) - RMS(x_{BWL T})}{RMS(x_{BWL T})} \quad (25)$$

In which, x_{BWBT} and $x_{BWL T}$ denote the deflection of bridge system with the BTMD and with the conventional linear TMD, respectively. Fig. 9 shows where BTMD improves the efficiency of the bridge control vibration system ($\eta > 0$) and where the conventional linear TMD has a better performance ($\eta < 0$).

Fig. 10(a) shows that there is a trajectory around the stable point of zero for the phase-plane diagram of the conventional linear TMD. As phase-plane diagram is shown in Fig. 10(b), there is a chaotic-like behavior for the BTMD system in which the trajectory surrounds the two stable equilibrium points and results the most optimal performance for the condition that the resonant amplification is assumed to be at any speed within a broadband input of vortex shedding velocity.

Finding the best location of installation for the BTMD is an important item that needs to be addressed for improving the effectiveness of the vibration control system. Fig. 11 illustrates a performance map in which the BTMD system is localized for the interior deck of the bridge. The main

challenges for developing an accurate BTMD for infrastructure systems are a detailed initial field vibration measurement and accurate design and manufacturing for the device.

5. Conclusions

In order to suppress vortex-induced vibration of suspension bridge deck, a bistable tuned mass damper (BTMD) mechanism was proposed in this paper. Design parameters of the nonlinear BTMD were optimized, and then the BTMD system got localized for the interior deck of the suspension bridge. Under two different wind load excitations of harmonic (sinusoidal) and broadband input of vortex shedding, optimization maps were obtained to pick a pair of optimal damping and nonlinear stiffness. For the case study, i.e., Kap Shui Mun Bridge, it was shown that we need extra damping and less nonlinear stiffness for the case of broad-band excitation against monochromatic load pattern. For the monochromatic loading pattern, a remarkable reduction factor of 37% was recorded for the BTMD against conventional TMD. The reason for that superior performance was found to be chaotic reciprocation of the dissipating mechanism between the two equilibrium positions. For the case of spectral loading, the optimal performance basins for the TMD and BTMD were obtained in the wind speed domain. It was shown that each control system has superior performance at specific range of the wind speeds. It was also found that the performance of the BTMD is very much dependent on the bending rigidity of the supports as well as the location of its installation and in our case found to be about 30% percent of the main span length from towers.

References

- Abdel-Rohman, M. and John, M.J. (2006), "Control of wind-induced nonlinear oscillations in suspension bridges using multiple semi-active tuned mass dampers", *J. Vib. Control*, **12**(9), 1011-1046. <https://doi.org/10.1177/1077546306069035>.
- Arena, A. and Lacarbonara, W. (2012), "Nonlinear parametric modeling of suspension bridges under aeroelastic forces: torsional divergence and flutter", *Nonlin. Dyn.*, **70**(4), 2487-2510. <https://doi.org/10.1007/s11071-012-0636-3>.
- Arioli, G. and Gazzola, F. (2017), "Torsional instability in suspension bridges: the Tacoma Narrows Bridge case", *Commun. Nonlin. Sci. Numer. Simul.*, **42**, 342-357. <https://doi.org/10.1016/j.cnsns.2016.05.028>.
- Andersen, M.S. and Brandt, A. (2018), "Aerodynamic instability investigations of a novel, flexible and lightweight triple-box girder design for long-span bridges", *J. Bridge Eng.*, **23**(12), 04018095. [https://doi.org/10.1061/\(ASCE\)BE.1943-5592.0001317](https://doi.org/10.1061/(ASCE)BE.1943-5592.0001317).
- Azzi, Z., Matus, M., Elawady, A., Zisis, I. and Irwin, P. (2018), "Large-scale aeroelastic testing to investigate the performance of span-wire traffic signals", *In Proc. 5th AAWE Workshop*, Miami, U.S.A. August.
- Battista, R. C. and Pfeil, M.S. (2000), "Reduction of vortex-induced oscillations of Rio-Niterói bridge by dynamic control devices", *J. Wind Eng. Ind. Aerod.*, **84**(3), 273-288. [https://doi.org/10.1016/S0167-6105\(99\)00108-7](https://doi.org/10.1016/S0167-6105(99)00108-7).
- Farhangdoust, S., Mehrabi, A. and Younesian, D. (2019), "Bistable wind-induced vibration energy harvester for self-powered wireless sensors in smart bridge monitoring systems", *In Nondestructive Characterization and Monitoring of Advanced Materials, Aerospace, Civil Infrastructure, and Transportation XIII* **10971**, 109710C. <https://doi.org/10.1117/12.2517424>.
- Farhangdoust, S. and Mehrabi, A. (2019), "Health monitoring of closure joints in accelerated bridge construction: A review of non-destructive testing application", *J. Advan. Concrete Technol.*, **17**(7), 381-404. <https://doi.org/10.3151/jact.17.381>.
- Fujino, Y. and Yoshida, Y. (2002), "Wind-induced vibration and control of Trans-Tokyo Bay crossing bridge", *J. Struct. Eng.*, **128**(8), 1012-1025. [https://doi.org/10.1061/\(ASCE\)0733-9445\(2002\)128:8\(1012\)](https://doi.org/10.1061/(ASCE)0733-9445(2002)128:8(1012))
- Gazzola, F. (2015), *Mathematical models for suspension bridges*. MS&A Springer.
- Guo, P., Li, S. and Wang, D. (2019), "Effects of aerodynamic interference on the iced straddling hangers of suspension bridges by wind tunnel tests", *J. Wind Eng. Ind. Aerod.*, **184**, 162-173. <https://doi.org/10.1016/j.jweia.2018.11.017>.
- Han, B., Yan, W.T., Cu, V.H., Zhu, L. and Xie, H.B. (2019), "H-TMD with hybrid control method for vibration control of long span cable-stayed bridge", *Earthq. Struct.*, **16**(3), 349-358. <https://doi.org/10.12989/eas.2019.16.3.349>.
- Harne, R.L. and Wang, K.W. (2013), "A review of the recent research on vibration energy harvesting via bistable systems", *Smart Mat. Struct.*, **22**(2), 023001. <https://doi.org/10.1088/0964-1726/22/2/023001>.
- Ghulam H., Mostafa R. and Shahin H. (2015), "Trade-off among mechanical properties and energy consumption in multi-pass friction stir processing of Al 7075-T651 alloy employing hybrid approach of artificial neural network and genetic algorithm", *Proc I Mech E Part B: J Eng. Manuf.*, **231**(1), 129-139.
- Ko, J.M., Sun, Z.G. and Ni, Y.Q. (2002), "Multi-stage identification scheme for detecting damage in cable-stayed Kap Shui Mun Bridge", *Eng. Struct.*, **24**(7), 857-868. [https://doi.org/10.1016/S0141-0296\(02\)00024-X](https://doi.org/10.1016/S0141-0296(02)00024-X).
- Larsen, A. and Larose, G.L. (2015), "Dynamic wind effects on suspension and cable-stayed bridges", *J. Sound Vib.*, **334**, 2-28. <https://doi.org/10.1016/j.jsv.2014.06.009>.
- Larsen, A., Esdahl, S., Andersen, J.E. and Vejrum, T. (2000), "Storebælt suspension bridge-vortex shedding excitation and mitigation by guide vanes", *J. Wind Eng. Ind. Aerod.*, **88**(2-3), 283-296. [https://doi.org/10.1016/S0167-6105\(00\)00054-4](https://doi.org/10.1016/S0167-6105(00)00054-4).
- Li, H., Laima, S., Zhang, Q., Li, N. and Liu, Z. (2014), "Field monitoring and validation of vortex-induced vibrations of a long-span suspension bridge", *J. Wind Eng. Ind. Aerod.*, **124**, 54-67. <https://doi.org/10.1016/j.jweia.2013.11.006>.
- Li, H., Laima, S., Ou, J., Zhao, X., Zhou, W., Yu, Y., and Liu, Z. (2011), "Investigation of vortex-induced vibration of a suspension bridge with two separated steel box girders based on field measurements", *Eng. Struct.*, **33**(6), 1894-1907. <https://doi.org/10.1016/j.engstruct.2011.02.017>.
- Li, Z., Feng, M.Q., Luo, L., Feng, D. and Xu, X. (2018), "Statistical analysis of modal parameters of a suspension bridge based on Bayesian spectral density approach and SHM data", *Mech. Syst. Signal Pr.*, **98**, 352-367. <https://doi.org/10.1016/j.ymssp.2017.05.005>.
- Leadenham, S. and Erturk, A. (2014), "M-shaped asymmetric nonlinear oscillator for broadband vibration energy harvesting: Harmonic balance analysis and experimental validation", *J. Sound Vib.*, **333**(23), 6209-6223. <https://doi.org/10.1016/j.jsv.2014.06.046>.
- Munir, A., Zhao, M., Wu, H., Ning, D. and Lu, L. (2018), "Numerical investigation of the effect of plane boundary on two-degree-of-freedom of vortex-induced vibration of a circular cylinder in oscillatory flow", *Ocean Eng.*, **148**, 17-32.

- <https://doi.org/10.1016/j.oceaneng.2017.11.022>.
- Nguyen, S.D., Halvorsen, E., and Jensen, G.U. (2013), "Wideband MEMS energy harvester driven by colored noise", *J. Microelectromech. Syst.*, **22**(4), 892-900. <https://doi.org/10.1109/JMEMS.2013.2248343>.
- Pellegrini, S.P., Tolou, N., Schenk, M. and Herder, J.L. (2013), "Bistable vibration energy harvesters: a review", *J. Intel. Mat. Syst. Struct.*, **24**(11), 1303-1312. <https://doi.org/10.1177/1045389X12444940>.
- Ranjbar, M., Boldrin, L., Scarpa, F., Neild, S. and Patsias, S. (2016), "Vibroacoustic optimization of anti-tetrachiral and auxetic hexagonal sandwich panels with gradient geometry", *Smart Mat. Struct.*, **25**(5), 054012. <https://doi.org/10.1088/0964-1726/25/5/054012>.
- Saha, A., Saha, P. and Patro, S.K. (2018), "Seismic protection of the benchmark highway bridge with passive hybrid control system", *Earthq. Struct.*, **15**(3), 227-241. <https://doi.org/10.12989/eas.2018.15.3.227>.
- Simiu, E. and Yeo, D. (2019), *Wind Effects on Structures: Modern Structural Design for wind*, Wiley-Blackwell.
- Simiu, E. (2011), *Design of Buildings for Wind: A Guide for ASCE 7-10 Standard Users and Designers of Special Structures*, John Wiley & Sons.
- Smith, I.J. (1980), "Wind induced dynamic response of the Wye bridge", *Eng. Struct.*, **2**(4), 202-208. [https://doi.org/10.1016/0141-0296\(80\)90001-2](https://doi.org/10.1016/0141-0296(80)90001-2).
- Soman, R., Kyriakides, M., Onoufriou, T. and Ostachowicz, W. (2018), "Numerical evaluation of multi-metric data fusion based structural health monitoring of long span bridge structures", *Struct. Infrastruct. Eng.*, **14**(6), 673-684. <https://doi.org/10.1080/15732479.2017.1350984>.
- Steinman, D.B. (1954), "Suspension bridges: The aerodynamic problem and its solution", *Am. Scientist*, **42**(3), 396-460.
- Tang, L. and Yang, Y. (2012), "A nonlinear piezoelectric energy harvester with magnetic oscillator", *Appl. Phys. Lett*, **101**(9), 094102. <https://doi.org/10.1063/1.4748794>.
- Vaz, D.C., Almeida, R. A. and Borges, A.R.J. (2018), "Wind action phenomena associated with large-span bridges", In *Bridge Engineering*. IntechOpen.
- Vocca, H., Neri, I., Travasso, F. and Gammaitoni, L. (2012), "Kinetic energy harvesting with bistable oscillators", *Appl. Energy*, **97**, 771-776. <https://doi.org/10.1016/j.apenergy.2011.12.087>.
- Wang, W., Cao, J., Bowen, C.R., Zhang, Y. and Lin, J. (2018), "Nonlinear dynamics and performance enhancement of asymmetric potential bistable energy harvesters", *Nonlinear Dyn.*, **94**(2), 1183-1194.
- Wang, W., Wang, X., Hua, X., Song, G. and Chen, Z. (2018), "Vibration control of vortex-induced vibrations of a bridge deck by a single-side pounding tuned mass damper", *Eng. Struct.*, **173**, 61-75. <https://doi.org/10.1016/j.engstruct.2018.06.099>
- Wang, L., Jiang, T.L., Dai, H.L. and Ni, Q. (2018), "Three-dimensional vortex-induced vibrations of supported pipes conveying fluid based on wake oscillator models", *J. Sound and Vib.*, **422**, 590-612. <https://doi.org/10.1016/j.jsv.2018.02.032>.
- Wu, T., Kareem, A. and Ge, Y. (2013), "Linear and nonlinear aeroelastic analysis frameworks for cable-supported bridges", *Nonlinear Dyn.*, **74**(3), 487-516.
- Xu, Y.L. (2018), "Making good use of structural health monitoring systems of long-span cable-supported bridges", *J. Civil Struct. Health Monit.*, **8**, 477-497.
- Younesian, D. and Alam, M.R. (2017), "Multi-stable mechanisms for high-efficiency and broadband ocean wave energy harvesting", *Appl. Energy*, **197**, 292-302. <https://doi.org/10.1016/j.apenergy.2017.04.019>.
- Zhang, Q.W., Chang, T.Y.P. and Chang, C.C. (2001), "Finite-element model updating for the Kap Shui Mun cable-stayed bridge", *J. Bridge Eng.*, **6**(4), 285-293. [https://doi.org/10.1061/\(ASCE\)1084-0702\(2001\)6:4\(285\)](https://doi.org/10.1061/(ASCE)1084-0702(2001)6:4(285)).
- Zhang X., Connor J. and Nepf H. (2012), "Wind Effect on Long Span Bridge". <http://hdl.handle.net/1721.1/74418>.
- Zhang, W., Wei, Z., Yang, Y. and Ge, Y. (2008), "Comparison and analysis of vortex induced vibration for twin-box bridge sections based on experiments in different reynolds numbers", *J. Tongji Uni*, **36**(1), 6.
- Zhou, G., Li, A., Li, J. and Duan, M. (2018), "Structural health monitoring and time-dependent effects analysis of self-anchored suspension bridge with extra-wide concrete girder", *Appl. Sci.*, **8**(1), 115. <https://doi.org/10.3390/app8010115>.
- Zhou, R., Ge, Y., Yang, Y., Du, Y. and Zhang, L. (2018), "Wind-induced nonlinear behaviors of twin-box girder bridges with various aerodynamic shapes", *Nonlin. Dyn.*, **94**(2), 1095-1115. <https://doi.org/10.1007/s11071-018-4411-y>.

CC